Deyl, Z., Macek, K., & Adam, M. (1979) *Biochem. Biophys. Res. Commun. 89*, 627–634.
Epstein, E. H. (1974) *J. Biol. Chem. 249*, 3225–3231.
Epstein, E. H., Scott, R. D., Miller, E. J., & Peiz, K. A., (1971) *J. Biol. Chem. 246*, 1718–1724.
Goldman, H. M. (1951) *J. Dent. Res. 30*, 331–336.
Hayashi T., & Nagai, Y. (1979) *J. Biochem. (Tokyo) 86*, 453–459.
Kresina, T. F., & Miller, E. J. (1979) *Biochemistry 18*, 3089–3097.
Laemmli, U. K. (1970) *Nature (London) 227*, 680–685.
Lichtenstein, J. R., Byers, P. H., Smith, B. D., & Martin, G. R. (1975) *Biochemistry 14*, 1589–1594.
Liotta, L. A., Abe, S., Robey, P. G., & Martin, G. R. (1979) *Proc. Natl. Acad. Sci. U.S.A. 76*, 2268–2272.
Miller, E. J., Finch, J. E., Chung, E., & Butler, W. T. (1976) *Arch. Biochem. Biophys. 173*, 631–637.
Narayanan, A. S., & Page, R. C. (1976) *J. Biol. Chem. 251*, 5464–5471.
Narayanan, A. S., Page, R. C., & Kuzan, F. (1978) *Lab. Invest. 39*, 61–65.
Narayanan, A. S., Hassell, T. M., Page, R. C., & Meyers, D. F. (1980) *J. Dent. Res. 59* (Special Issue A), 343.
Page, R. C., & Shreoder, H. E. (1973) *Int. Dent. J. 23*, 455–469.
Page, R. C., & Ammons, W. F. (1974) *Arch. Oral Biol. 19*, 651–658.
Page, R. C., & Schroeder, H. E. (1976) *Lab. Invest. 33*, 235–249.
Page, R. C., Ammons, W. F., Schectman, L. R., & Dillingham, L. A. (1974) *Arch. Oral Biol. 19*, 1039–1043.
Rhodes, R. K., & Miller, E. J. (1978) *Biochemistry 17*, 3442–3448.
Sage, H., & Bornstein, P. (1979) *Biochemistry 18*, 3815–3821.
Studier, F. W. (1973) *J. Mol. Biol. 79*, 237–248.
Uitto, J. (1979) *Arch. Biochem. Biophys. 192*, 371–379.
Welsh, C., Gay, S., Rhodes, R. K., Pfister, R., & Miller, E. J. (1980) *Biochim. Biophys. Acta* (in press).

Conformational Dynamics of Insulin in Solution. Circular Dichroic Studies†

Y. Pocker* and Subhasis B. Biswas

ABSTRACT: Conformational changes of bovine insulin in solution with concentration and pH detected by circular dichroic (CD) studies are reported. The change in the CD spectrum of insulin in the higher concentration range (from 100 μM down to 2 μM) is relatively small, but in the lower concentration range (from 2 μM down to 60 nM) the CD spectrum changes substantially with concentration. A detailed analysis of the data indicates that the hormone has two major conformational states: conformation I, a form which predominates in extremely dilute solutions and corresponds to the monomeric state, and conformation II, a form present in the crystalline state and also, with but minor changes, in all associated states in solution. The apparent conformation of insulin at various concentrations is computed by using a nonlinear least-squares iterative computer program. The mean residue ellipticities at 223 and 208 nm are extrapolated by using $[\theta]_\lambda$ vs. $f_{monomer}$ plots to calculate the conformations of monomeric and dimeric insulin. These calculations indicate that conformation I of insulin has 21% less helix content than conformation II, the latter conformation being very similar to that found in the crystalline state. It is also evident from these calculations that the conformational transition is of the helix–coil type. Studies pertaining to the dependence of the CD spectrum of insulin on pH are also reported, and a comparison is made with earlier sedimentation coefficient studies. An analysis of the data indicates that changes in the sedimentation coefficient correspond quite closely to changes of CD spectra with pH. This paper is the first report known to us pertaining to conformational studies of insulin in the monomeric state; it presents evidence for conformational transitions of the protein hormone induced by concentration and pH. Since insulin is biologically active mainly in the monomeric state, a knowledge of its conformation in this state should be an important tool in deciphering the molecular basis of insulin action.

At the present time the effects of insulin in biological systems are reasonably well-known, but the mechanism of action is still not well understood. Recent studies indicate that the first step in the action of insulin is its binding to a receptor site on the cell membrane (Cuatrecasas, 1974; Freychet, 1976; Kahn, 1975; Roth et al., 1975). This binding alters the transmembrane transport processes, and the dynamics of binding in turn depend on the conformation of protein hormone in solution.

In the last few years, several groups have investigated the conformation of insulin in the crystalline form and in solution (Blundell et al., 1971; Dodson et al., 1979; Goldman & Carpenter, 1974; Peking Insulin Structure Research Group, 1974; Wood et al., 1975). Through these studies, the structure of insulin in the crystalline state is now known at a resolution of 1.5 Å. The conformation of insulin in the solution is still not fully delineated.

Insulin exhibits a complex association behavior in crystal and in solution. In the crystalline state it exists as a hexamer and in solution it exists as an equilibrium mixture of monomers, dimers, tetramers, hexamers, and possibly some higher associated states. The studies on the association behavior of insulin by equilibrium sedimentation (Goldman & Carpenter, 1974; Jeffrey & Coates, 1965, 1966; Pekar & Frank, 1972) indicate that under physiological conditions this protein hormone must exist exclusively as a monomer. So far, the conformation of insulin in the monomeric state has not been studied and, therefore, is totally unknown.

† From the Department of Chemistry, University of Washington, Seattle, Washington 98195. *Received March 6, 1980.* Support of this research by grants from the National Institute of Arthritis, Metabolism and Digestive Diseases of the U.S. Public Health Service and by the National Science Foundation is gratefully acknowledged. A part of this paper has been presented (Biswas & Pocker, 1979).

0006-2960/80/0419-5043$01.00/0

Goldman & Carpenter (1974) reported small concentration-dependent changes in the circular dichroic (CD)[1] spectra of insulin in the concentration range 500–2.5 μM. Their observation was later confirmed by the work of Wood et al. (1975). However, a 2.5 μM solution still contains significant amounts of dimers, tetramers, and hexamers. Although these observations indicate a possible relationship between circular dichroic spectra and the association behavior of insulin, it proved difficult to decide whether the CD changes are in fact due to conformational changes. In an effort to resolve this problem, we recorded CD spectra of bovine insulin over a wide range of concentrations (from 100 μM down to 60 nM) in a Jobin Yvon Circular Dichrograph III apparatus. The major changes in CD spectra take place between 2 μM and 60 nM. The 60 nM insulin solution is >98% monomeric. We made corrections for a small dimer population in order to calculate the conformation of monomeric insulin. The average helix contents of insulin at various concentrations were calculated from the mean residue ellipticities at 223 nm using $[\theta]_{223}$ for 100% helix to be -25.1×10^3 deg cm^2 dmol^{-1}. The overall conformations of insulin at various concentrations were computed by using a nonlinear least-squares iterative program following the method of Chen et al. (1974).

Fredericq & Neurath (1950) and Fredericq (1953, 1956) in their unique studies on the molecular weight of insulin have shown that the sedimentation coefficient ($s_{20,w}$) and the weight-average molecular weight ($M_{w,app}$) of insulin depend on pH and salt concentration. It is evident from their accurate studies that the association of insulin depends on the net charge on the protein molecule which in turn depends on the pH of the solution and its ionic strength. Significantly, it is reported that the in vitro binding of insulin to its plasma membrane receptor is extremely sensitive to the pH of the medium and a maximal binding is observed around pH 8.0 (Freychet et al., 1973; Roth et al., 1975). In diabetic ketoacidosis the biological activity of insulin is known to be reduced due to the decrease of pH in the blood. These interesting reports led us to study the effect of pH on the CD spectra of insulin.

Experimental Procedures

Materials

Insulin. Bovine Zn–insulin was purchased from Sigma Chemical Co. (Lot No. 47C-0264). Zn-free insulin hydrochloride was prepared by the method of Goldman & Carpenter (1974).

Solutions. All solutions were prepared with deionized and redistilled water and analytical reagent grade KH_2PO_4 and K_2HPO_4. The buffer used was 0.005 M phosphate buffer. The pH was adjusted with 1 N HCl. Concentrations of insulin solutions were determined spectrophotometrically in a Cary 14 spectrophotometer by using a molar extinction coefficient, $\epsilon_{278} = 6.2 \times 10^3$ M^{-1} cm^{-1} at pH 7.0 and 25 °C. In fact, the molar extinction coefficient of this protein depends on concentration (Rupley et al., 1967) so that our initial measurements were always made on stock solutions containing 100 μM insulin. Other solutions were prepared by dilution of the stock solution. In the pH-dependence study, 100 μM solutions were prepared with 0.05 M glycine–0.05 M NaCl and 1.0 N HCl (acidic pH) or 1.0 N NaOH (basic pH). The 100 nM solutions were prepared with 0.005 M phosphate buffer–0.05 M NaCl and adjusted with 1 N HCl or 1 N NaOH.

Methods

Circular Dichroic Measurements. All CD spectra were recorded on a Jobin Yvon Dichrograph Mark III instrument in which a high-frequency elasto-optic modulator is used in place of pockel cells used in older instruments. The Jobin Yvon Dichrograph Mark III has extremely high sensitivity (0.03 mdeg/mm) and a high signal to noise ratio.

Calibration. The circular dichrograph was calibrated by using 0.002 M *d*-10-camphorsulfonic acid (Eastman Kodak Co.). The *d*-10-camphorsulfonic acid was purified by recrystallization from hot acetic acid followed by sublimation. The $\Delta\epsilon$ value for *d*-10-camphorsulfonic acid was taken as +2.37 at 290 nm (Fasman, 1975). All sensitivities were separately calibrated at different time constants.

Measurements. All spectra were recorded at pH 7.0 or as specified and at 25 °C. Above 100 nM the spectra were recorded in the usual manner. At extreme dilutions, however, spectra were recorded by artificially suppressing the dynode voltage, which also alters the calibrations. The accuracy of the measurements was maintained by continuous calibration with 0.002 M *d*-10-camphorsulfonic acid solution. The $[\theta]_\lambda$ values reported are the average of three to nine measurements. Cells used were of far-UV quartz and 1–100-mm path lengths.

The mean residue ellipticities were calculated by the expression

$$[\theta]_\lambda = 3300\Delta\epsilon = 3300\left(\frac{ds}{N_R ml}\right)$$

where d = extension recorded in millimeters, s = calibrated sensitivity, N_R = number of amino acid residues in the protein molecule, m = concentration in moles per liter, and l = path length of the cell in centimeters. All $[\theta]_\lambda$ values are expressed in deg cm^2 dmol^{-1}.

Determination of Monomer Content. The plot of $M_{w,app}$ vs. concentration reported by Goldman & Carpenter (1974) was available to us, and we used this plot for estimating monomer content.

Goldman and Carpenter considered the equilibria

$$I \underset{-I}{\overset{+I}{\rightleftharpoons}} I_2 \underset{-I_2}{\overset{+I_2}{\rightleftharpoons}} I_4 \underset{-I_2}{\overset{+I_2}{\rightleftharpoons}} I_6 \qquad (K_{12},\ K_{24},\ K_{46})$$

where values of K_{12}, K_{24}, and K_{46} are $K_{12} = 2.22 \times 10^5$ M^{-1}, $K_{24} = 40$ M^{-1}, and $K_{46} = 220$ M^{-1}. These values were calculated from apparent $M_{w,app}$ values. Instead of using these constants, we used $M_{w,app}$ values for the determination of monomer content at different concentrations. In the lower concentration range we considered a simple monomer–dimer equilibrium, because the concentrations of tetramer, hexamer, and other higher associated states are negligible. We obtained $M_{w,app}$ values from the $M_{w,app}$ vs. C plot of Goldman & Carpenter (1974), and the fractions of the total amount of insulin in the monomeric state ($f_{monomer}$) at different concentrations were calculated in the following way:

$$M_{w,app} = \frac{M_1C_1 + M_2C_2}{C_1 + C_2}$$

where $M_{w,app}$ = the apparent weight-average molecular weight, M_1 = molecular weight of the monomers, M_2 = molecular weight of the dimers, C_1 = concentration of the monomers, and C_2 = concentration of the dimers. So, $f_{monomer}$ can be expressed in terms of the equation:

$$f_{monomer} = 1 - \frac{2M_1}{4M_1 - M_{w,app}}$$

Calculation of Helix Content. The far-ultraviolet circular dichroic spectrum of a protein depends on its conformation.

[1] Abbreviation used: CD, circular dichroism.

Table I: Concentration-Dependent Circular Dichroic Data, Association Parameters and Average Helix Content of Insulin[a]

concn (μM)	$-[\Theta]_{223} \times 10^{-3}$ [b]	$-[\Theta]_{208} \times 10^{-3}$ [b]	$[\Theta]_{208}/[\Theta]_{223}$	$-[\Theta]_{273}$	$M_{w,app}$ [c]	$f_{monomer}$ [d]	av helix content[e] (%)
100	10.6 ± 0.2	13.4 ± 0.2	1.26	198	12400	0.0	42
10	10.3 ± 0.2	12.8 ± 0.2	1.25	171	10500	0.092	41
5	9.9 ± 0.2	12.7 ± 0.2	1.27	170	10200	0.124	39
2	9.7 ± 0.3	12.8 ± 0.3	1.22	150	9100	0.260	38
1	8.8 ± 0.3	12.6 ± 0.4	1.42	104	7800	0.470	35
0.75	8.3 ± 0.4	12.5 ± 0.5	1.51		7600	0.570	33
0.50	7.8 ± 0.4	11.9 ± 0.6	1.52		7000	0.700	31
0.25	6.7 ± 0.6	10.4 ± 0.6	1.59		6200	0.850	28
0.10	6.6 ± 0.8	10.0 ± 0.8	1.52		5950	0.930	26
0.06	6.2 ± 0.8	10.1 ± 0.8	1.62		5850	0.960	25

[a] At pH 7 in 0.005 M phosphate buffer at 25 °C. [b] The unit of mean residue ellipticities is deg cm^2 dmol^{-1}. The signal to noise ratio and reproducibility are indicated in the error limit. [c] $M_{w,app}$ = the apparent weight-average molecular weight (Goldman & Carpenter, 1974). [d] $f_{monomer}$ = fraction of the total amount of insulin in monomeric state. [e] Average helix content refers to weight-average helix content of insulin at a particular concentration. See text for experimental details and methods of calculation.

Several groups proved that the approximate conformation of a protein can be estimated by analyzing its CD spectrum (Sarkar & Doty, 1966; Greenfield & Fasman, 1969; Fasman et al., 1970; Saxena & Wetlaufer, 1971; Chen et al., 1972, 1974). Following the method of Chen et al. (1972, 1974), we analyzed the CD spectra by a least-squares iterative computer program which estimates the gross conformation of a protein in terms of α-helix, β-sheet, and random coil structures. This essentially neglects some finer structures of proteins like turn regions or short α-helical or β-sheet segments. However, this analysis offers a better understanding of the conformational dynamics of a protein in solution. Chen et al. (1972, 1974) showed that the CD spectrum of a protein can be expressed in terms of eq 1 where $f_H + f_\beta + f_R = 1$ and all f's ≥ 0.0. The

$$[\Theta]_\lambda = f_H[\Theta]^H_\lambda + f_\beta[\Theta]^\beta_\lambda + f_R[\Theta]^R_\lambda \quad (1)$$

$[\Theta]_\lambda$ is the experimental mean residue ellipticity at wavelength λ (in nanometers), and $[\Theta]^H_\lambda$, $[\Theta]^\beta_\lambda$, and $[\Theta]^R_\lambda$ are the theoretically computed values from the X-ray studies of nine different proteins (of which one is insulin) for 100% helix, 100% β sheet, and 100% random coil, respectively. The f's are the fractions of helix (f_H), β sheet (f_β), and random coil (f_R). Chen et al. (1974) used a chain length dependent factor k as $[\Theta]^H_\lambda$ depends on the average number of residues per helix ($\bar{n}$) so the expression will be eq 2. The $[\Theta]^{H(\infty)}_\lambda$ in eq 2 is the

$$[\Theta]^H_\lambda = f_H[\Theta]^{H(\infty)}_\lambda[1 - (k/\bar{n})] + f_\beta[\Theta]^\beta_\lambda + f_R[\Theta]^R_\lambda \quad (2)$$

theoretical mean residual ellipticity of a 100% helical protein with infinite chain length. This is a nonlinear equation, and, by use of $(1 - f_H - f_\beta)$ for f_R, the f_H, f_β, f_R, and $\bar{n}$ can be calculated by a nonlinear iterative least-squares computer program. We used a revised version of nonlinear iterative least-squares program BMD 07R on a CDC 6400 computer at the Computer Center of the University of Washington.

The $[\Theta]_\lambda$ values were calculated at 3-nm wavelength intervals between 204 and 243 nm. All conformations reported are weight-average conformations of all species (monomers, dimers, tetramers, hexamers, etc.) present in the solution.

Alternatively, we used a simpler way to estimate the helix content of insulin from CD spectrum. An examination of the computed spectra of α helix, β sheet, and random coil of Chen et al. (1974) shows that the contribution of β sheet and random coil to the mean residue ellipticity at 223 nm of a protein is very small and can be neglected.

The $[\Theta]_{223}$ values for monomer and dimer were extrapolated from Figure 5. The $[\Theta]_{223}$ for dimer is -11.30×10^3 and that for monomer is -6.07×10^3. If we assume that in the dimer the conformation of insulin is similar to that in the crystals, then the dimer contains ~45% helix, so the theoretical value

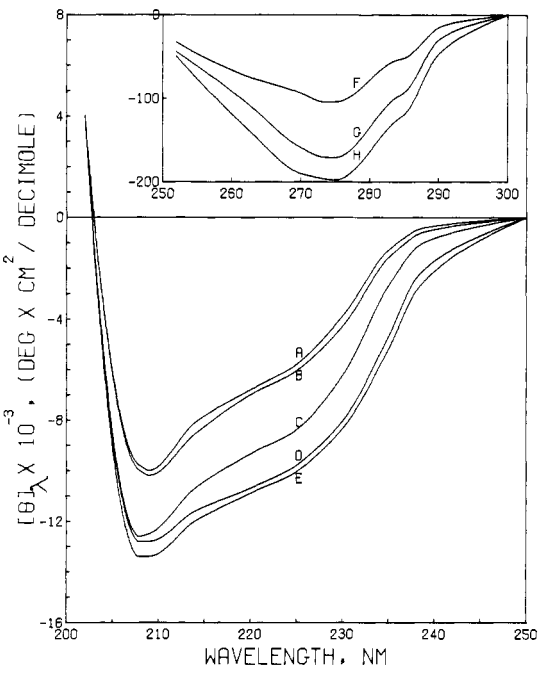

FIGURE 1: Concentration-dependent far-ultraviolet (200–250 nm) circular dichroic spectra of bovine insulin at (A) 100 nM, (B) 250 nM, (C) 500 nM, (D) 1.0 μM, and (E) 100 μM. All solutions are made with 0.005 M phosphate buffer. (Insert) Concentration-dependent near-ultraviolet (250–300 nm) circular dichroic spectra of bovine insulin at (F) 1.0 μM, (G) 10.0 μM, and (H) 100 μM. For details of the experiment, see Experimental Procedures.

of $[\Theta]^H_{223}$ for the insulin dimer is $(-11.3 \times 10^3)/0.45 = -25.10 \times 10^3$. The helix contents of insulin at various concentrations were calculated by dividing the observed $[\Theta]_{223}$ by -25.1×10^3 deg cm^2 dmol^{-1} (Table I). The results of this method are in fair agreement with the results of nonlinear least-squares iterative analysis.

Results

Concentration-Dependent CD of Insulin. The near- and far-ultraviolet circular dichroic spectra of insulin at various concentrations are given in Figure 1. The mean residue ellipticities at 208 nm and 223 nm are given in Table I.

In the near-ultraviolet region (250–300 nm), ellipticity at 273 nm decreases with decreasing concentration. The change between 100 μM and 10 μM is small but, between 10 μM and 1.0 μM, substantial changes take place. The $-[\Theta]_{273}$ decreases from 198 at 100 μM to 104 at 1.0 μM. This is the lowest concentration at which measurement is possible. Below this concentration measurement is difficult due to the noise

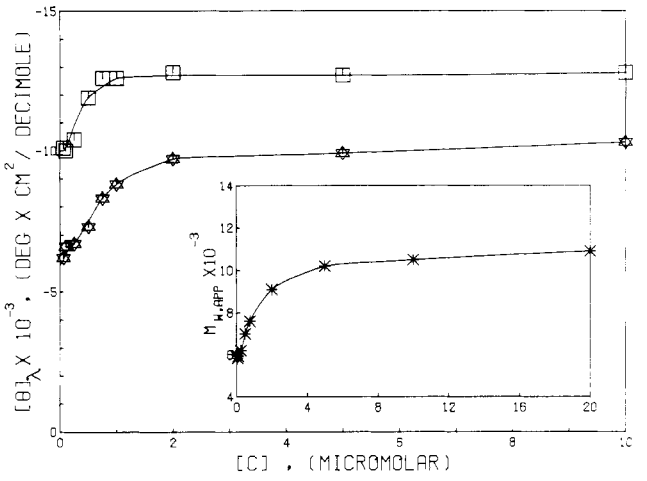

FIGURE 2: Plot of $-[\Theta]_\lambda$ vs. C at λ = 208 nm (□) and λ = 223 nm (☆). (Insert) Plot of $M_{w,app}$ vs. C. For experimental details, see Goldman & Carpenter (1974).

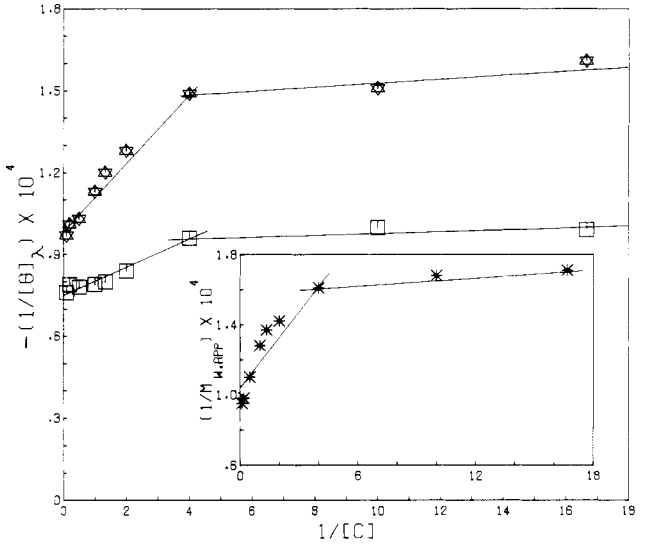

FIGURE 3: Plot of $-1/[\Theta]_\lambda$ vs. $1/C$ at λ = 208 (□) and λ = 223 nm (☆). (Insert) Plot of $1/M_{w,app}$ vs. $1/C$.

problem. These results are in good agreement with the results of previous workers (Goldman & Carpenter, 1974; Strickland & Mercola, 1976; Wood et al., 1975).

In the far-ultraviolet region ellipticities at 223 and 208 nm decrease with concentration. A substantial change in $[\Theta]_\lambda$ takes place between 2 μM and 60 nM (Figure 1). The change in $[\Theta]_\lambda$ between 100 μM and 2 μM is small. The $-[\Theta]_{223}$ of a 100 μM solution is 10.6×10^3, a value which decreases to 6.2×10^3 for a 60 nM solution. The $[\Theta]_{208}$ changes in a similar fashion, but the changes are relatively small. The $-[\Theta]_{208}$ changes from 13.4×10^3 at 100 μM to 10.1×10^3 at 60 nM solution. The $[\Theta]_{208}$ and $[\Theta]_{223}$ were plotted against concentration in Figure 2. Both of these plots are similar in nature. The plot of apparent weight-average molecular weight ($M_{w,app}$), reported by Goldman & Carpenter (1974), vs. concentration (C) (Figure 2, insert) is hyperbolic and in the proper concentration range (60 nM to 20 μM) is closely comparable to the plots of $[\Theta]_\lambda$ vs. C in Figure 2. The ratios of $[\Theta]_{208}/[\Theta]_{223}$ are given in Table I. It is interesting to note that, while $-[\Theta]_{208}$ and $-[\Theta]_{223}$ both decrease with decreasing concentration, the ratio $[\Theta]_{208}/[\Theta]_{223}$ increases with decreasing concentration. The average rate of change of $[\Theta]_{208}$ is less than that of $[\Theta]_{223}$. This observation is similar to that reported by Wood et al. (1975).

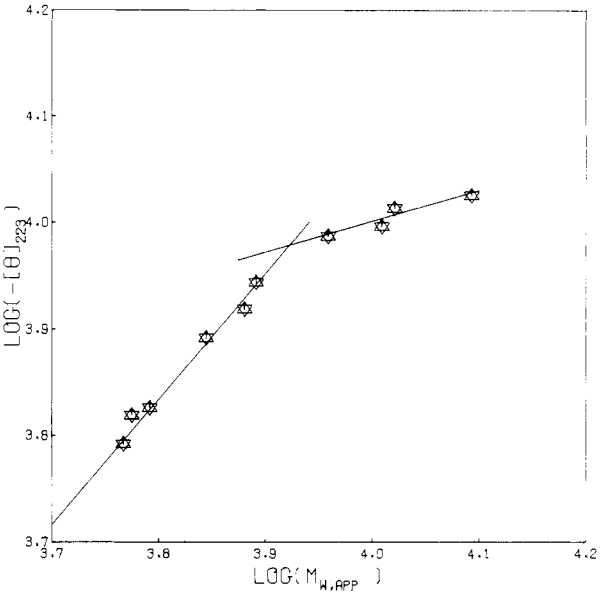

FIGURE 4: Plot of log $-[\Theta]_{223}$ vs. log $M_{w,app}$.

Table II: Extrapolated Values for Monomer and Dimer[a]

associated state	$-[\Theta]_{223} \times 10^{-3}$ [b]	$-[\Theta]_{208} \times 10^{-3}$ [c]	$[\Theta]_{208}/[\Theta]_{223}$	% helix
monomer	6.07	9.90	1.63	24.2
dimer	11.30	15.00	1.35	45.0

[a] The experimental conditions are same as those in Table I. [b] Mean residue ellipticity at 223 nm in deg cm² dmol⁻¹. [c] Mean residue ellipticity at 208 nm in deg cm² dmol⁻¹.

Since the $[\Theta]_\lambda$ vs. C plots are hyperbolic in nature, the plots $-1/[\Theta]_\lambda$ vs. $1/C$ should give straight lines. The $-1/[\Theta]_\lambda$ vs. $1/C$ plots are shown in Figure 3. Plots for both λ = 223 nm and λ = 208 nm have inflection points around 250 nM where the slopes of the plots decrease substantially.

The double-reciprocal plot of $1/M_{w,app}$ vs. $1/C$ (Figure 3, insert) is similar to that of $-1/[\Theta]_\lambda$ vs. $1/C$ plot with an inflection point near 250 nM. These plots on examination reveal certain important features of concentration-dependent circular dichroism of insulin in solution. Between 100 μM and 250 nM these double-reciprocal plots have closely comparable slopes, but below 250 nM these plots reach a plateau. This striking correlation between $[\Theta]_\lambda$ and $M_{w,app}$ led us to critically analyze the relation between association behavior of insulin and its circular dichroic behavior. In an attempt to decipher the relationship between the association behavior and CD of insulin explicitly, we plotted log $-[\Theta]_{223}$ vs. log $M_{w,app}$ (Figure 4). This plot shows a linear relationship between $[\Theta]_{223}$ and $M_{w,app}$ in the lower concentration range (0–1.0 μM) where monomer–dimer equilibrium exists. At higher concentrations formation of other associated states like tetramer and hexamer is evident from this plot.

The monomer content of an insulin solution at a particular concentration is expressed as a fraction of the total amount of insulin in the monomeric state ($f_{monomer}$) and the values of $f_{monomer}$ at different concentrations are given in Table I. The plots of $-[\Theta]_{208}$ and $-[\Theta]_{223}$ vs. $f_{monomer}$ are shown in Figure 5. Both plots are straight lines showing the direct dependence of $[\Theta]_\lambda$ on the monomer content of insulin solution. The slight deviation from the straight line in the higher concentration range is due to the neglect of tetramer and hexamer concentration in this region. The theoretical $[\Theta]_\lambda$ values for monomer and dimer were evaluated from these plots. The extrapolated values of $[\Theta]_{208}$ and $[\Theta]_{223}$ are given in Table II. These

Table III: Conformation of Insulin at Various Concentrations Calculated by Nonlinear Least-Squares Method

concn (μM)	% helix	% β sheet	% random coil
100	40	18	42
10	36	16	48
1	27	24	49
0.25	23	21	56
0.10	22	22	56

extrapolated values appear suitable for estimating the secondary structure of insulin in the monomeric state.

Conformational Analysis. The helix contents of insulin at various concentrations were calculated by the simpler method, and the values are given in Table I. The average helix content in the crystal is 45%, a value which decreases to 25%, at 60 nM concentration, so the total decrease in helix content is ~20%, according to this calculation.

The computation of secondary structures (average) at different concentration by nonlinear least-squares iterative analysis gives a detailed picture of the conformational changes. The conformations at various concentrations are given in Table III.

This analysis indicates approximately an 18% decrease in helix content, a 4% increase in β-sheet content, and a 14% increase in random coil content, when the concentration decreases from 100 μM to 100 nM; hence, the transformation is basically a transition of the helix–coil type.

Our estimation of secondary structures and nonlinear least-squares analysis estimation are closely comparable. The extrapolated $[\Theta]_{223}$ values for the monomeric and dimeric states are -6.07×10^3 and -11.30×10^3, respectively (Table II), which correspond to 24.2 and 45% helical conformation. So the two conformational states of insulin are (1) conformation I, observed in the monomeric state, containing approximately 24% helix, 20% β sheet, and 56% random coil, and (2) conformation II, observed in the higher associated states and in the crystalline state, containing 45% helix, 12% β sheet, and 43% random coil as reported by Blundell et al. (1971) and the Peking Insulin Structure Research Group (1974).

Effect of pH. In our study of the effect of pH on the CD of insulin, we observed a change in $[\Theta]_{223}$ in the basic pH range (7.0–11.2) at 100 μM and 100 nM concentration (Table IV and Figure 6). The buffer strength in 100 nM solutions was kept lower to decrease dynode voltage and to raise the signal to noise ratio. The $[\Theta]_{223}$ of a 100 μM solution at pH 7.0 is -10.76×10^3, a value which changes to -8.8×10^3 at pH 11.2. But for a 100 nM solution the change in $[\Theta]_{223}$ is from -6.7×10^3 at pH 7.0 to -6.33×10^3 at pH 11.2. A comparison of the pH dependence of the $[\Theta]_{223}$ of 100 μM solution and

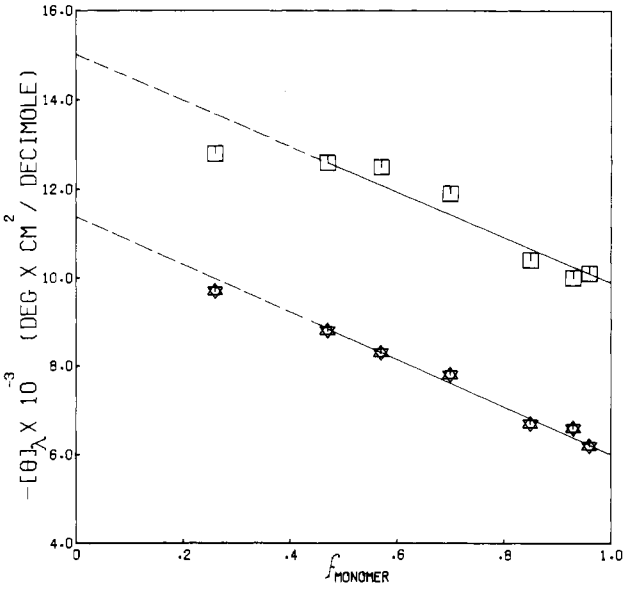

FIGURE 5: Plot of $-[\Theta]_\lambda$ vs. $f_{monomer}$. Extrapolation of $[\Theta]_{223}$ and $[\Theta]_{208}$ for insulin in monomeric and dimeric states. For details, see the text.

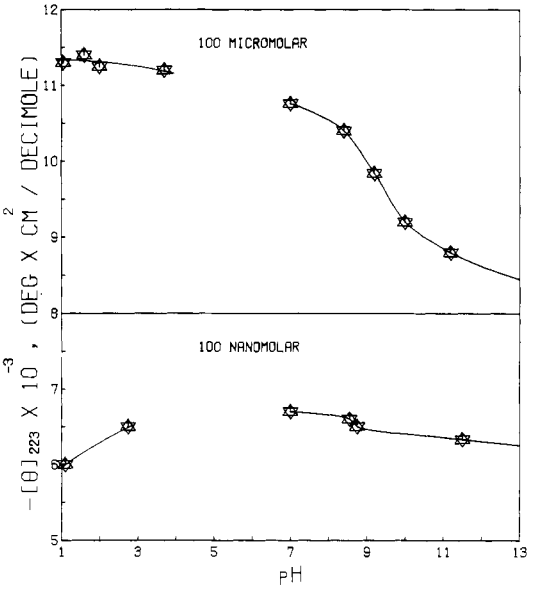

FIGURE 6: Plot of $-[\Theta]_{223}$ vs. pH at 100 μM concentration (above) and at 100 nM concentration (below). For experimental details, see Experimental Procedures.

100 nM solution shows that the change in $[\Theta]_{223}$ with pH for a 100 nM solution is significantly smaller than the corresponding change for a 100 μM solution. In the acidic pH range, the measurements were done at lower pH since the

Table IV: Effect of pH on Circular Dichroism of Insulin[a]

				(I) 100 μM[b]					
pH	1.05	1.6	2.0	3.7	7.0	8.4	9.2	10.0	11.2
$-[\Theta]_{208} \times 10^{-3}$	13.9	14.0	14.0	14.1	13.6	13.5	13.7	14.0	14.1
$-[\Theta]_{223} \times 10^{-3}$	11.3	11.4	11.25	11.2	10.76	10.4	9.84	9.2	8.8
$[\Theta]_{223}/[\Theta]_{208}$	0.813	0.814	0.810	0.800	0.791	0.770	0.718	0.657	0.624
% helix	45.0	45.4	44.8	44.6	42.9	41.4	39.2	36.6	35.0
				(II) 100 nM[c]					
pH	1.1	2.75	7.0	8.55	8.75	11.5			
$-[\Theta]_{208} \times 10^{-3}$	11.4	12.9	12.92	11.6	13.2				
$-[\Theta]_{223} \times 10^{-3}$	6.00	6.50	6.70	6.60	6.50	6.33			
$[\Theta]_{223}/[\Theta]_{208}$	0.526	0.504	0.519	0.569	0.500				
% helix	23.9	25.8	26.7	26.3	25.8	25.2			

[a] For experimental conditions see text. [b] The error in measurements is ±0.01 for pH and ±0.400 for $[\Theta]_\lambda$. [c] The error in measurements is ±0.01 for pH and ±0.900 for $[\Theta]_\lambda$.

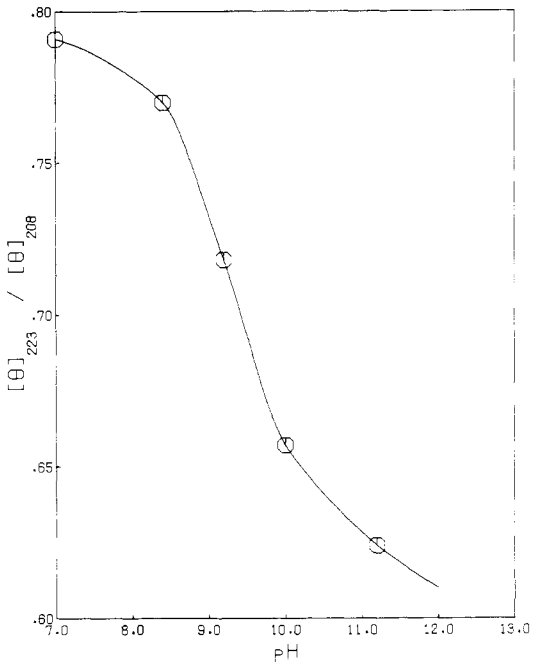

FIGURE 7: Plot of $[\theta]_{223}/[\theta]_{208}$ vs. pH.

Table V: Conformations of Insulin at Different pH Values[a]

pH	% helix	% β sheet	% random coil
2.0	44.9	14.1	41.0
7.0	42.0	17.1	40.9
11.2	29.0	21.6	49.4

[a] For experimental conditions see text.

measurements were difficult in the neighborhood of isoelectric point of insulin. The $[\theta]_{223}$ of 100 μM solution remains constant (-11.3×10^3) in the acidic pH range. In 100 nM solution the $[\theta]_{223}$ decreases slightly with decreasing pH.

The large change in $[\theta]_{223}$ of a 100 μM solution with increasing pH (above 7.0) is due to a dissociation of the higher associated states to monomers as a consequence of high charge repulsion. The slight decrease of $[\theta]_{223}$ of a 100 nM solution with increasing pH may be due to either a small dimer population or minor conformational changes. Significantly the ratio $[\theta]_{223}/[\theta]_{208}$ for a 100 μM solution decreases with pH in the same fashion as does $[\theta]_{223}$ itself (Table IV and Figure 7).

The average helix contents at different values of pH are calculated and presented in Table IV. In 100 μM solution in the acidic pH range, the helix content is similar to that observed in the crystalline state and in dimer, according to our computation. But it decreases with increasing pH. In 100 nM solution there is only a slight variation in helix content, which is negligibly small. The conformations of 100 μM solutions at pH 2.0, 7.0, and 11.2 are computed by least-squares iterative analysis, a treatment which gives a more accurate picture of the average conformations at different pH values (Table V). With increasing pH, helix content decreases with a concurrent increase in random-coil content and with a slight increase in β-pleated sheet content.

Discussion

Several groups have studied the circular dichroic behavior of insulin in solution (Goldman, 1971; Goldman & Carpenter, 1974; Mercola et al., 1967; Menêndes & Herskovits, 1970; Wood et al., 1975). Goldman & Carpenter (1974) and Wood et al. (1975) reported that the CD spectrum of insulin in both near- and far-ultraviolet region changes with concentration in the range from 500 μM down to 2.5 μM. The association constant for the dimerization of insulin is very high [2.22×10^5 M^{-1} (Goldman & Carpenter, 1974); 4.0×10^4 M^{-1} (Lord et al., 1973); 7.5×10^5 M^{-1} (Y. Pocker and S. B. Biswas, unpublished results)] so that these studies were carried out in solution in which insulin dimers predominate.

The measurements reported in the present study have been done over a wide concentration range (100 μM to 60 nM) down to extreme dilutions, where insulin exists almost entirely as a monomer. Our study uncovered some interesting information about the structure of insulin in the monomeric state, which could be extremely important in the structure–activity correlation of insulin and its derivatives.

We observed substantial changes in the CD spectra with dilution. The change in CD between 100 and 2 μM concentration is small, similar to that observed by Goldman & Carpenter (1974) and Wood et al. (1975). The $[\theta]_{223}$ changes from -10.6×10^3 at 100 μM to -9.7×10^3 at 2 μM. However, since in a 2 μM solution, insulin is largely dimeric, our investigations were extended down to more dilute solutions. Below 2 μM the CD of insulin changes appreciably down to 250 nM with a $[\theta]_{223}$ of -6.7×10^3. Below 250 nM the change is small due to the small amount of dimer. It proved possible to record spectra down to a 60 nM solution, though with increasing noise problems at very low concentrations. The $[\theta]_{223}$ reaches a value of -6.2×10^3 at 60 nM solution. The overall change in $[\theta]_{223}$ is 4.4×10^3. Such a large change may be ascribed either (1) to general conformational changes of all insulin species or (2) to the specific formation of insulin monomer, a species whose concentration is steadily increasing with dilution and whose conformational state is totally different from that present in its associated forms in solution. To resolve this dilemma, we compared the circular dichroic behavior of insulin with its association behavior. The $[\theta]_\lambda$ vs. C plot in Figure 2 is closely comparable to the weight-average molecular weight ($M_{w,app}$) vs. C plot from the data of Goldman & Carpenter (1974) (Figure 3, insert) in the concentration range 0–20 μM. The double-reciprocal plots of $-1/[\theta]_\lambda$ vs. $1/C$ given in Figure 3 and $1/M_{w,app}$ vs. $1/C$ in the insert of Figure 3 have comparable slopes and inflection points around 250 nM, indicating that below 250 nM the solution is essentially monomeric and its composition does not change significantly. The most convincing evidence for the relation of CD with the association behavior comes from the log $-[\theta]_\lambda$ vs. log $M_{w,app}$ plot in Figure 4. In the lower concentration region, 0–1.0 μM, the plot displays a linear relationship between $[\theta]_{223}$ and $M_{w,app}$. But a deviation is noted above 1.0 μM which is simply due to the formation of tetramers and other associated states. Thus, the rate of change of $[\theta]_{223}$ remains smaller than that of $M_{w,app}$, which is understandable if $[\theta]_{223}$ values corresponding to dimers, tetramers, and other associated states are similar or only slightly different. These observations lead us to propose that the conformation of insulin in the monomeric state is different from that which exists in the dimer, tetramer, hexamer, and other possible associated states. Our thesis then is that insulin has two major conformational states, (1) conformation I, a form associated with monomeric insulin and present in very dilute solutions (≤60 nM), i.e., under physiological conditions in blood and probably in certain insulins and their derivatives which lack associative capacity, e.g., guinea pig insulin and desoctapeptide (B_{23-30}) insulin, and (2) conformation II, a form present in dimer, tetramer, hexamer, and other associated states as well as in crystalline form. The

conformational state II is very nearly the crystalline conformation: it has 45% helix, 12% β sheet, and 43% random coil (Blundell et al., 1971). Our calculations indicate a 24% helical, 21% β-sheet, and 55% random coil structure for the monomeric state. Clearly, I and II represent flexible conformations whose detailed spatial geometries depend upon pH, ionic strength, and metal ion concentration.

The dimer to monomer dissociation process is, therefore, associated with a conformational transition involving a 21% decrease in the helix content of the protein molecule, an 8% increase of β-sheet content, and a 13% increase in random coil content. Insulin in the crystalline state has B_9–B_{20} amino acid residues in a very rigid α-helical structure and A_1–A_4 residues in a loosely helical turn, and its A_{12}–A_{19} residues are helical. Out of these three helical regions in insulin structure only the last two A-chain helical regions can undergo helix–coil type transitions because of their less compact structure. The α helix comprising of B_9–B_{20} residues is very compact and well protected by neighboring regions of the protein; it will be consequently less susceptible to solvent perturbation.

Circular dichroic measurements have also been carried out with porcine insulin. The corresponding spectra differ somewhat from those of the bovine hormone. Values of $-[\Theta]_{223}$ at 100 μM and 100 nM of porcine insulin are 10.2×10^3 and 7.2×10^3, respectively; the corresponding $-[\Theta]_{208}$ values are 12.6×10^3 and 10.8×10^3. Insulins from both bovine and porcine sources display similar conformational behavior in solution and in crystal. For the crystal, Blundell et al. (1971) reported the existence of conformational asymmetry arising from differences in the two monomeric units that form the dimer. Later, Bentley et al. (1978) delineated the extensive structural differences between rhombohedral $2Zn^{2+}$ and $4Zn^{2+}$ insulin crystals and further showed that the two crystalline forms can be interconverted. Clearly, the occurrence of considerable flexibility in the restrictive medium of the crystalline lattice and its dependence on metal ion and salt concentration is most instructive. In this regard it is interesting to note that our studies indicate that in solution insulin exhibits complex conformational dynamics which depend on pH and the concentrations of protein, metal ion, and salt.

Effect of pH. The CD of insulin changes with pH. In the pH range from 1.1 up to 3.7, the $[\Theta]_{223}$ of 100 μM insulin remains practically unchanged with a value of -11.3×10^3, which is equal to the theoretical value of $[\Theta]_{223}$ for the dimer. The major decrease of the mean residue ellipticity at 223 nm starts around physiological pH of 7.4 and steadily decreases with increasing pH. Fredericq (1956) showed that the sedimentation coefficient $s_{20,w}$ of a 435 μM insulin solution decreases with increasing pH and $s_{20,w}$ at very low pH corresponds to the calculated sedimentation coefficient of the dimer. Therefore, the change in the CD spectrum of insulin in the pH range 7.0–11.2 is due to the dissociation of dimers into monomers. A nonlinear least-squares iterative computational analysis of the pH-dependent CD spectra of insulin indicates an 18% decrease of α-helix content when the pH of the insulin solution increases from 7.0 to 11.2. Both $-[\Theta]_{223}$ vs. pH (Figure 6) and $[\Theta]_{223}/[\Theta]_{208}$ vs. pH (Figure 7) plots show a midpoint around pH 9.3. These titrations indicate that the dissociation of dimers to monomers is due to the deprotonation of certain amino acid residues in insulin exhibiting an apparent pK_a of 9.3, which results in a net anionic charge repulsion.

Acknowledgments

We thank Dr. Ronald E. Chance of Eli Lilly Co. and Dr. E. Schlichtkrull of NOVO Research Institute, Denmark, for their generous gifts of various insulins.

References

Bentley, G., Dodson, G., & Lewitova, A. (1978) *J. Mol. Biol. 126*, 871–875.

Biswas, S. B., & Pocker, Y. (1979) 34th Northwest Regional Meeting of the American Chemical Society, June 13–15, Richland, Washington, Abstr. 92, American Chemical Society, Washington, D.C.

Blundell, T. L., Cutfield, J. F., Cutfield, S. M., Dodson, E. J., Dodson, G. G., Hodgkin, D. C., Mercola, D. A., & Vijayan, M. (1971) *Nature (London) 231*, 506–511.

Chen, Y. H., Yang, J. T., & Martinez, H. (1972) *Biochemistry 11*, 4120–4131.

Chen, Y. H., Yang, J. T., & Chan, K. H. (1974) *Biochemistry 13*, 3350–3359.

Cuatrecasas, P. (1974) *Annu. Rev. Biochem. 43*, 169–214.

Dodson, E. J., Dodson, G. G., Hodgkin, D. C., & Reynolds, C. D. (1979) *Can. J. Biochem. 57*, 469–479.

Fasman, G. D., Ed. (1975) *Handbook of Biochemistry and Molecular Biology*, Vol. 3, CRC Press, Cleveland, OH.

Fasman, G. D., Hoving, H., & Timasheff, S. (1970) *Biochemistry 9*, 3316–3324.

Fredericq, E. (1953) *Nature (London) 171*, 570–571.

Fredericq, E. (1956) *Arch. Biochem. Biophys. 65*, 218–228.

Fredericq, E., & Neurath, H. (1950) *J. Am. Chem. Soc. 72*, 2684–2691.

Freychet, P. (1976) *Diabetologia 12*, 83–100.

Freychet, P., Kahn, C. R., Roth, J., & Neville, D. M., Jr. (1973) *Int. Cong. Ser.-Excerpta Med. No. 256*, 335.

Goldman, J. (1971) Ph.D. Thesis, University of California, Berkeley, CA.

Goldman, J., & Carpenter, F. H. C. (1974) *Biochemistry 13*, 4567–4574.

Greenfield, N., & Fasman, G. D. (1969) *Biochemistry 8*, 4108–4116.

Jeffrey, P. D., & Coates, J. H. (1965) *Biochim. Biophys. Acta 109*, 551–556.

Jeffrey, P. D., & Coates, J. H. (1966) *Biochemistry 5*, 489–498.

Kahn, C. R. (1975) *Methods Membr. Biol. 3*, 81–146.

Lord, R. S., Gubensek, F., & Rupley, J. A. (1973) *Biochemistry 12*, 4385–4390.

Menêndez, C. J., & Herskovits, T. T. (1970) *Arch. Biochem. Biophys. 103*, 286–294.

Mercola, D. A., Morris, J. W. S., Arquilla, E. R., & Bromer, W. W. (1967) *Biochim. Biophys. Acta 133*, 224–232.

Pekar, A. H., & Frank, B. H. (1972) *Biochemistry 11*, 4013–4016.

Peking Insulin Structure Research Group (1974) *Sci. Sin. (Engl. Ed.) 17*, 752.

Roth, J., Kahn, C. R., Lesniak, M. A., Gorden, P., DeMeyts, P., Megyesi, K., Neville, D. M., Jr., Gavin, J. R., III, Soll, A. H., Freychet, P., Goldfine, I. D., Bar, R. S., & Archer, J. A. (1975) *Recent Prog. Horm. Res. 31*, 95–139.

Rupley, J. A., Renthal, R. D., & Praissman, M. (1967) *Biochim. Biophys. Acta 140*, 185–187.

Sarkar, P. K., & Doty, P. (1966) *Proc. Natl. Acad. Sci. U.S.A. 55*, 981–989.

Saxena, I. P., & Wetlaufer, D. B. (1971) *Proc. Natl. Acad. Sci. U.S.A. 68*, 969–972.

Strickland, E. H., & Mercola, D. A. (1976) *Biochemistry 15*, 3875–3884.

Wood, S. P., Blundell, T. L., Wollmer, A., Lazarus, N. R., & Neville, R. W. J. (1975) *Eur. J. Biochem. 55*, 531–542.